The Gray-Thornton Model of Granular Segregation

Michael Shearer*, Lindsay B. H. May*, Nicholas Giffen* and Karen E. Daniels†

*Department of Mathematics, NC State University, Raleigh, NC, USA
†Department of Physics, NC State University, Raleigh, NC, USA

Abstract. In this paper, we explore properties of the Gray-Thornton model for particle size segregation in granular avalanches. The model equation is a single conservation law expressing conservation of mass, driven by shear and gravity, for the concentration of the smaller of two types of particle in a bidisperse mixture. Sharp interfaces across which the concentration jumps are shock wave solutions of the partial differential equation. We show that they can form internally from smooth data, as well as propagate in from boundaries of the domain. We prove a general stability result that expresses the physically reasonable notion that an interface should be stable if and only if the concentration of small particles is larger below the interface than above. Once shocks form, they are sheared by the flow, leading to loss of stability when an interface becomes vertical. The subsequent evolution of a mixing zone, a two-dimensional rarefaction solution of the equation that replaces the unstable part of the shock can be tracked explicitly for a short time. We conducted experiments to test the continuum model against real flow in a Couette geometry, in which a bidisperse mixture is confined in the annular region between concentric vertical cylinders. Initially, the material is placed in the annulus with a layer of large particles below a layer of small particles. The sample is then sheared by rotating the bottom confining plate, while a heavy top plate is allowed to move vertically to accommodate Reynolds dilatancy. Comparison to predictions of the model show reasonable agreement with both the mixing and resegregation rates. However, the model naturally fails to capture short-time dilatancy, finite size effects, or three-dimensional effects.

Keywords: Segregation,granular materials,shock waves,hyperbolic conservation laws

INTRODUCTION

Granular materials have a tendency to segregate by size when set in motion. The classic paper of Savage and Lun [10] gives an explanation of this phenomenon for a bidisperse mixture of particles of different size but the same density, in the context of steady chute flow. The Savage and Lun model is based on quantifying the mechanisms of kinetic sieving and squeeze-expulsion. More recently, Gray and Thornton [4] formulated a time-dependent continuum model using mixture theory, incorporating the crucial role of gravity in kinetic sieving.

In this paper, we consider the Gray-Thornton model in two space variables (x,z), and time t, where x corresponds to distance down an incline, and z is a height variable, so that gravity is in the direction of decreasing z. The model is a scalar conservation law describing the evolution of the concentration $\varphi(x,z,t)$ of small particles as the material is sheared by a given depth-dependent velocity $u(z)$ in the x-direction. The concentration φ is the fraction of the solid material consisting of small particles, so that $1-\varphi$ is the concentration of large particles. The velocity $u(z)$, assumed to be time-independent, transports particles down the slope, and induces segregation through the shear rate $u'(z)$. The Gray-Thornton equation takes the form

$$\varphi_t + u(z)\varphi_x + (S\varphi(\varphi-1))_z = 0, \qquad -\infty < x < \infty,\ -1 < z < 1,\ t > 0, \tag{1}$$

In this equation, segregation is driven by the normal velocity of small particles, taken to be proportional to the concentration $1-\varphi$ of large particles. The constant of proportionality S is a segregation rate and sets the time scale. In avalanche flow, the parallel velocity $u(z)$ is roughly linear, and a constant segregation rate is a reasonable assumption. However, for shear induced through a boundary, such as provided by a moving confining plate, the velocity is known to be more closely exponential than linear [9]. In this circumstance, segregation occurs significantly faster in regions of high shear than in those with low shear rate, so that S is properly taken to be a function of z.

Properties of equation (1) and related models have been explored in a series of papers [3, 8, 12]. Equation (1) is a simple macroscopic model for segregation, a complicated dynamic process at the grain diameter scale. Moreover, it is a continuum model that seeks to approximate fluid-like flow of a granular material in a context in which flow typically occurs only within a depth of a small number grains. Nonetheless, the model captures several features of segregation under shear.

The scalar equation (1) has some unusual features that create novel solution patterns. The structure of the equation is that it transports particles parallel to the x-axis with a speed that is linearly depth dependent, giving a non-constant coefficient in the transport term. As a consequence, characteristics are curved. A more subtle effect of the non-constant coefficient is seen on shock waves. These are interfaces in space-time across which the solution has a jump discontinuity. We show in this paper that shocks are stable if there is a greater concentration of large particles above the shock than below. The novel feature that appears in solutions is that, because of the shearing, stable shock waves can become vertical, and then lose stability. The emerging solution structure is still not fully understood, but in this paper we report on some progress in understanding what happens immediately after the shock loses stability.

In [6, 7], we considered equation (1) with exponential function $u(z)$ and $S(z) = s|u'(z)|$. However, we restricted attention to solutions independent of x, mimicking conditions in a Couette cell in which layers of large and small particles are sheared by rotating a lower confining plate. In the final section of this paper, we summarize results from analysis of this modified equation, and comparison to experimental results. Considering that the model is very simple, and does not account for finite size effects, it is remarkable that it can capture qualitative features of mixing and resegragation in the experiments. With only one free parameter (setting the time scale), the model is able to achieve agreement with the different rates of mixing and segregation quantified in the experiment.

In the next section, we consider a general equation

$$\varphi_t + u(z)\varphi_x + (S(z)f(\varphi))_z = 0, \qquad -\infty < x < \infty,\ -1 < z < 1,\ t > 0, \tag{2}$$

Here, $f(\varphi)$ models segregation normal to the x-axis. We assume it is a smooth convex function on the interval $0 \le \varphi \le 1$, with $f(0) = f(1) = 0$, consistent with the idea that the normal flux of small particles should be zero if there are either no large particles or no small particles at that location.

CHARACTERISTICS AND SHOCKS

In this section, we present the basic building blocks of solutions of equation (2), and prove a very general stability result. We write equation (2) as

$$\varphi_t + u(z)\varphi_x + S(z)f'(\varphi)\varphi_z = -S'(z)f(\varphi) \tag{3}$$

If the solution $\varphi(x,z,t) = \varphi_0$ is known at the point $x = x_0, z = z_0$, and time $t = t_0$, then the PDE shows how to continue the solution to $t > t_0$, by tracing the solution along *characteristics,* given by the ODE system

$$\begin{gathered} \frac{dx}{dt} = u(z); \quad \frac{dz}{dt} = S(z)f'(\varphi); \quad \frac{d\varphi}{dt} = -S'(z)f(\varphi); \\ x(t_0) = x_0;\ z(t_0) = z_0;\ \varphi(x_0,z_0,t_0) = \varphi_0. \end{gathered} \tag{4}$$

Since the final two ODE are independent of x, they form a vector field in the (z,φ)-plane, with a first integral:

$$S(z)f(\varphi) = \text{const.} \tag{5}$$

In particular, when $\varphi = \varphi(z,t)$ is independent of x, this equation is a useful representation of characteristics.

Shock waves are smooth surfaces $z = \hat{z}(x,t)$ across which $\varphi(x,z,t)$ has a jump discontinuity. Let $\varphi_\pm(x,t) = \varphi_(x,\hat{z}(x,t)\pm,t)$. Since equation (2) is in divergence (i.e., conservative) form in space-time, the normal component of the divergence-free function $(\varphi, u(z)\varphi, S(z)f(\varphi))$ is continuous across the shock:

$$\hat{z}_t[\varphi] + \hat{z}_x u(\hat{z})[\varphi] - S(\hat{z})[f(\varphi)] = 0. \tag{6}$$

Here, we have used the normal $(\hat{z}_t, \hat{z}_x, -1)$ at the shock; the notation $[g(\varphi)] = g(\varphi_+) - g(\varphi_-)]$ signifies the jump of a function $g(\varphi)$ across the shock. Consequently, the evolution of the shock, coupled to that of the weak solution $\varphi(x,z,t)$ on either side of it, is given by the PDE

$$\hat{z}_t + u(\hat{z})\hat{z}_x = S(\hat{z})G(\varphi_+, \varphi_-), \tag{7}$$

where

$$G(\varphi_+,\varphi_-) = \begin{cases} \dfrac{f(\varphi_+) - f(\varphi_-)}{\varphi_+ - \varphi_-}, & \varphi_+ \ne \varphi_- \\ f'(\varphi_-), & \varphi_+ = \varphi_-. \end{cases} \tag{8}$$

This equation can be solved by the method of characteristics, once $\varphi_\pm(x,t)$ are known. More generally, these functions are found in conjunction with the evolution of the shock wave, as in [1]. To assess stability of the shock in the sense of hyperbolic conservation laws, we use the Lax entropy condition which ensures that, for a given initial condition with a shock, the solution can be continued at least for a short time with the same structure. That is, the solution φ evolves, and the shock evolves with it. The Lax entropy condition stipulates that the shock is stable if the characteristic surfaces that would emanate from points on the shock immediately overlap. As a consequence, the solution would be double-valued in the overlapping region, but in fact well-posedness is recovered by constructing a shock lying within the region, and satisfying (7). This construction is standard in the hyperbolic equations literature [11] when the solution is constant along characteristics; it corresponds to *structural* stability (i.e., short-time persistence) of the solution rather than the *asymptotic* (i.e., long-time) stability, commonly referred to in dynamical systems.

Stability of shocks

Since φ is not constant along characteristics, the treatment of stability is not completely standard. Nonetheless, for a stable shock, the two characteristic surfaces in space-time overlap, and the single-valuedness of the solutions has to be recovered by continuing the shock into this region.

We suppose there is a shock wave $z = \hat{z}(x,t)$, with well-defined values of φ on either side at time $t = t_0$. Let $\varphi^0_\pm(x) = \varphi_\pm(x,t_0)$.

Theorem 1 *The interface $z = \hat{z}(x,t)$ is dynamically stable if $\varphi^0_+ < \varphi^0_-$; it is unstable if $\varphi^0_+ > \varphi^0_-$.*

Proof: The idea of stability is that the characteristic surfaces generated by characteristics orginating on the shock at time $t = t_0$, with initial conditions $\varphi = \varphi^0_\pm$, should overlap for small $t > t_0$, so that a shock can be fit in between, satisfying the Rankine-Hugoniot condition. To verify this condition, we calculate the speeds of the two characteristic surfaces, and of the shock, normal to the shock at time $t = t_0$. The normal $\hat{N}$ to the shock $z = \hat{z}(x,t)$ is given by

$$\hat{N} = (-\hat{z}_x, 1)/(1+\hat{z}_x^2)^{1/2}. \tag{9}$$

The characteristic speeds $\lambda_\pm$ normal to the shock are given by

$$\lambda_\pm = (x', z').\hat{N}, \tag{10}$$

where $x'(t), z'(t)$ are given by the characteristic equations (4). Thus,

$$\lambda_\pm = \frac{1}{(1+\hat{z}_x^2)^{1/2}} \left(-u(\hat{z})\hat{z}_x + S(\hat{z}) f'(\varphi_\pm)\right). \tag{11}$$

The velocity of the shock at fixed $x = x_0$ is given by $(\dot{x}, \dot{z}) = (0, \hat{z}_t)$. Thus, the normal speed σ is given by

$$\sigma = \hat{N} \cdot (\dot{x}, \dot{z}) = \hat{z}_t/(1+\hat{z}_x^2)^{1/2}. \tag{12}$$

Now, $\hat{z}(x,t)$ satisfies the PDE (7), so that

$$\hat{z}_t = -u(\hat{z})\hat{z}_x + S(\hat{z}) G(\varphi_+, \varphi_-).$$

Substituting into (12), we find

$$\sigma = \frac{1}{(1+\hat{z}_x^2)^{1/2}} \left(-u(\hat{z})\hat{z}_x + S(\hat{z}) G(\varphi_+, \varphi_-)\right). \tag{13}$$

Comparing (11) and (13), we see that, from convexity of $f(\varphi)$, $\lambda_- > \sigma > \lambda_+$ is equivalent to $\varphi_+ < \varphi_-$, as claimed. ■

Shock formation

In this section, we examine the tendency of shocks to form in the interior of the flow. Shock formation is associated with finite-time blow-up of the gradient of the solution, so that the slope of the graph becomes infinite as a shock forms.

Thus, it makes sense to examine the evolution of the gradient $\nabla\varphi(x,z,t) = (\varphi_x, \varphi_z)$ in a smooth solution $\varphi(x,z,t)$. We do this by differentiating the PDE (2) with respect to x and z :

$$\frac{dv}{dt} = -S(z)f''(\varphi)vw - S'(z)f'(\varphi)v \tag{14a}$$

$$\frac{dw}{dt} = -u'(z)v - S(z)f''(\varphi)w^2 - 2S'(z)f'(\varphi)w - S''(z)f(\varphi). \tag{14b}$$

The derivatives on the left hand side are along characteristics, but note that both z and φ evolve along the characteristics, so that in general, the system of ODE has to include the characteristic equations. In general, this is a complicated system to analyze, and complete results are not available. However, we can treat special cases. For the original Gray-Thornton model, in which $u(z)$ is linear, and $S(z) > 0$ is constant, a complete characterization of shock formation is given in [1]. Here, we consider the case of exponential $S(z)$, which is consistent with the experimental configuration described below. Specifically, we assume

$$u'(z) > 0; \quad S(z) = se^{\beta(z+1)}, \quad -1 \le z \le 1, \tag{15}$$

with $s > 0$ constant. We prove the following result.

Theorem 2 *Suppose the conditions (15) hold. If $\varphi_x^0(x_0,z_0) \ge 0$, and $\varphi_z^0(x_0,z_0) < 0$, then either a shock forms in finite time, or the characteristic emanating from (x_0,z_0) reaches a boundary $z = \pm 1$ before $\nabla\varphi$ becomes singular.*

Proof: First, observe that the w-axis $v = 0$ is invariant for equation (14a). In case (a), it follows from the assumption $v(0) = \varphi_x^0(x_0,z_0) > 0$, that $v(t) > 0$ for all $t > 0$ for which the solution of (14) remains bounded. This is the only information we need concerning v in case (a) in order to analyze finite time blow-up of w in equation (14b).

Differentiating equation (5), we obtain

$$S'(z)f'(\varphi)w = -\frac{S'(z)^2}{S}f(\varphi) \tag{16}$$

Substituting into equation (14b), we get,

$$\frac{dw}{dt} = -S(z)f''(\varphi)w^2 + \left(\frac{S'(z)^2}{S(z)} - S''(z)\right)f(\varphi) - u'(z)v < -S(z)f''(\varphi)w^2, \tag{17}$$

since $v > 0$, $\frac{S'(z)^2}{S(z)} - S''(z) = s\beta^2 e^{\beta(z+1)} > 0$ and $f(\varphi) \le 0$. Now z and φ are evolving on the characteristic emanating from (x_0,z_0), but both $S(z) > 0$ and $f''(\varphi) > 0$ are bounded from below by positive constants, in the physical domain $-1 < z < 1, 0 \le \varphi \le 1$. Thus, there is $k > 0$ such that

$$\frac{dw}{dt} < -kw^2, \tag{18}$$

at least until the characteristic reaches the boundary.

Since $w(0) = \varphi_z^0(x_0,z_0) < 0$, then (18) implies that $w(t) \to -\infty$ in finite time, since

$$w(t) \le \frac{w(0)}{1 + kw(0)t}.$$

■

Remarks: 1. The conditions of the theorem relate to the orientation of contours of φ initially. Under these conditions, a larger concentration of smaller particles lies below and to the right of a mixture with a higher concentration of larger particles. As the sample is sheared, the large particles migrate upwards, and smaller particles downwards, thereby narrowing the spread of contours, eventually forming a sharp interface across which the particle concentrations jump.

2. If $w(0) = \varphi_z^0(x_0,z_0) > 0$, then the dynamics are somewhat more complicated, with the contours of φ rolling over as $w(t) = \varphi_z$ changes sign. Once this happens, the conditions of the theorem are satisfied, and a shock forms. However, to prove this rigorously, we would need to establish that $w(t^*) < 0$ for some finite time $t = t^*$, in order to show that $w(t) \to -\infty$. The evolution of $w(t)$ is controlled by $v(t)$:

$$\frac{dw}{dt} < -u'(z)v. \tag{19}$$

Now, $u'(z) \geq k_0 = \min_{-1\leq z\leq 1}\ u'(z) > 0$. Provided $v(t) > 0$ is bounded away from $v = 0$, then $w(t)$ crosses the v-axis in finite time.

3. In the simpler case of the original Gray-Thornton model, in which $u(z)$ is linear, $S(z)$ is constant, and $f(\varphi) = \varphi(\varphi - 1)$, system (14) simplifies considerably. Solutions φ are constant on characteristics, and the various terms that are now constants rather than variable can be eliminated from the equations by scaling, leaving the system

$$\frac{dv}{dt} = -2vw \tag{20a}$$

$$\frac{dw}{dt} = -v - 2w^2. \tag{20b}$$

Somewhat surprisingly, this system can be solved explicitly:

$$v(t) = \frac{v_0}{q(t)}, \quad w(t) = \frac{w_0 - v_0 t}{q(t)}, \quad q(t) = 1 + 2w_0 t - v_0 t^2, \tag{21}$$

where $v(0) = v_0, w(0) = w_0$. Consequently, conditions for shock formation can be specified precisely, and the time at which the shock forms can be expressed exactly in terms of the initial conditions [1]: shocks form if and only if $q(t)$ has a positive zero.

Shock breaking

Once a shock wave forms, it evolves according to the PDE (7), as discussed above. In this subsection, we show that certain shocks lose stability, due to being sheared by the flow. To avoid the complicated problem of how the solution evolves on either side of the shock, let's simplify the issue. In fact, let's take $\varphi_+ = 0, \varphi_- = 1$, so that the shock is stable. Then $G(\varphi_+, \varphi_-) = 0$ in equation (7). Furthermore, if we take $u(z) = z$, the original form of the Gray-Thornton model, then (7) becomes the inviscid Burgers equation [13] for the shock location $z = \hat{z}(x,t)$:

$$\hat{z}_t + \hat{z}\hat{z}_x = 0. \tag{22}$$

Now solutions of Burgers equation are known to break in finite time, unless they are monotonically increasing. Consequently, any shock wave solution satisfying (22) will become vertical in finite time if $\hat{z}_x < 0$ anywhere, at any time. This makes sense, because the interface is being sheared by the depth-dependent velocity. In the classical theory of Burgers equation, the solution can be continued as a shock wave, but here, the solution itself is a shock, and as it breaks, it loses stability because a middle section is now unstable: it has $\varphi+ < \varphi_-$, but because the section has turned over, $\varphi = \varphi_+ = 0$ *below* the shock, and $\varphi = \varphi_- = 1$ *above* the shock. (See Theorem 1.)

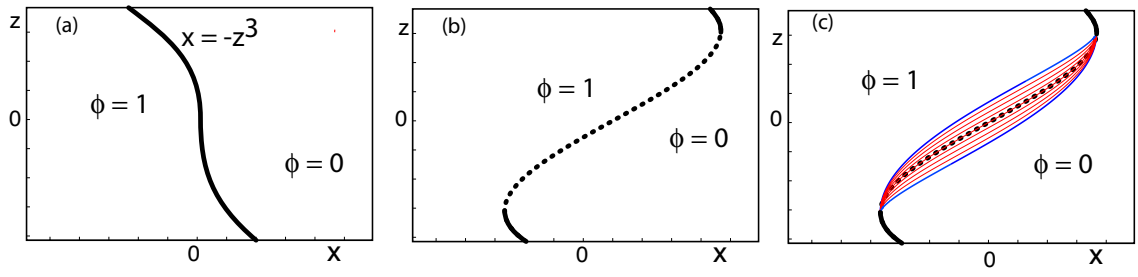

FIGURE 1. Solutions of (1), with $u(z) = z$ and initial condition (23). (a) Initial condition. (b) Evolved shock showing unstable section. (c) Solution with rarefaction wave, $t < 1/12$.

The solution is in fact continued using the method of characteristics to introduce a rarefaction wave, corresponding to a mixing zone. Consider an initial condition

$$\varphi(x,z,0) = \begin{cases} 1, & x < -z^3, \\ 0, & x > -z^3. \end{cases} \tag{23}$$

in which the interface $x = -z^3$ is already vertical at $z = 0$ in the initial condition. Then to see the shock breaking, it is convenient to consider the parameterization of the shock by z rather than x: $x = \hat{x}(z,t) = -z^3 + zt$ satisfies the evolution equation for $\hat{x}$:

$$\hat{x}_t + z\hat{x}_z = 0. \tag{24}$$

Then for $t > 0$, $\hat{x}(z,t)$ is non-monotonic; it is increasing between $z = \pm\sqrt{\frac{t}{3}}$, the unstable section of the evolved shock wave, and decreasing outside this interval. The solution with a rarefaction wave is valid for $t < \frac{1}{12}$, and is shown in Fig. 1. Beyond $t = \frac{1}{12}$, the solution becomes more complicated, but can be calculated with a simple numerical algorithm, as described in a forthcoming paper [1].

EXPERIMENTS WITH A COUETTE CELL

Experiments were conducted in an annular Couette cell, in which a mixture of small and large particles were sheared between concentric vertical cylinders. Here, we summarize results that will appear in a pair of papers [6, 7]. The experimental setup and protocol are described in detail in [2]. A bottom confining plate is rotated at constant frequency $f = 49 \pm 0.5$ mHz, approximately 3 rpm, and a top plate exerts a controlled pressure on the particles $(0.36 \pm 0.008)\,mg$, where mg is the total weight of the particles and the variation in force is due to the stretching of springs partially supporting the plate. The top plate is free to move vertically, thereby accommodating dilation and consolidation. Experiments reported here were carried out with particles that are spherical glass beads, of diameters 3 mm and 6 mm. Different size ratios, and variations in other experimental conditions are described in [2].

The apparatus allows us to compare quantitatively predictions of the Gray-Thornton model with experimental data. We find that the model captures the gross behavior of mixing and segregation as the material is sheared, even though it cannot reproduce significant features of the flow. To reflect conditions in the experiments, we make several assumptions concerning the model. First, we assume that, although mixing and segregation involve three-dimensional motion of particles, we consider solutions that depend only on the vertical variable z. This assumption is reflected in the initial configurations chosen for the experiments, in which a layer of small particles is placed above a layer of large particles. Second, we assume that the segregation rate is proportional to the shear rate, reflecting the notion that there should be more segregation when the sample is sheared faster. As the particles mix, they occupy significantly less volume, so that the top plate falls slightly. Later, as the mixture resegregates, they begin to occupy more volume, and the top plate rises. We assume that the degree of segregation is measured by the position of the top plate. The connection between model solutions and the experiments can be provided by a mapping between local concentration and the packing density.

In the experiment, we take two types of measurements. From high speed images we extract particle trajectories, which lead to an average velocity profile $u(z)$ that is roughly independent of time and φ. The second measurement is to record the position $H(t)$ of the top plate as a function of time t.

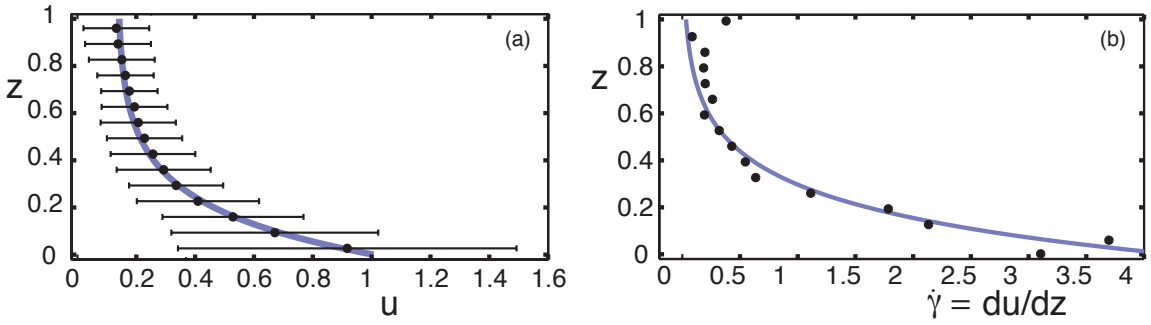

FIGURE 2. (a) Measured velocity profile $u(z)$ (•) in the region $0 \le z \le 1$, showing the exponential fit to the shear rate data in (b). Velocities are scaled so that $u(0) = 1$. (b) Shear rate $\dot{\gamma} = |du/dz|$ within the region $0 \le z \le 1$. The solid line is the fit to an exponential function.

Fig. 2(a) summarizes averaged velocity data, and a fit by an exponential function $u(z)$. The horizontal bars indicate the spread of the data, using the width of a parabolic fit at half height. In Fig. 2(b), we show the corresponding shear rate plot and fit by the exponential function $|u'(z)|$. Near the top (resp. bottom) of the cell, a layer of large (resp. small) particles forms quickly, creating an effective boundary. Consequently, the velocity profile and shear rate are determined from data in the middle section shown in the figure, normalized to $0 \le z \le 1$. It is worth noting that the shear rate $\dot{\gamma}$ is non-zero everywhere, establishing that the material is in a fluid-like flowing state at all times, even away from the rotating lower boundary. The exponential shear rate is used in solving the initial value problem

$$\begin{aligned} \varphi_t + s(u'(z)\varphi(1-\varphi))_z &= 0, \quad 0 < z < 1,\ t > 0 \\ \varphi(z,0) &= \begin{cases} 0, & 0 < z < 0.5 \\ 1, & 0.5 < z < 1, \end{cases} \end{aligned} \tag{25}$$

with boundary conditions $\varphi(0,t) = 1, \varphi(1,t) = 0$. As mentioned earlier, the segregation parameter $s > 0$ sets the time scale for the evolution.

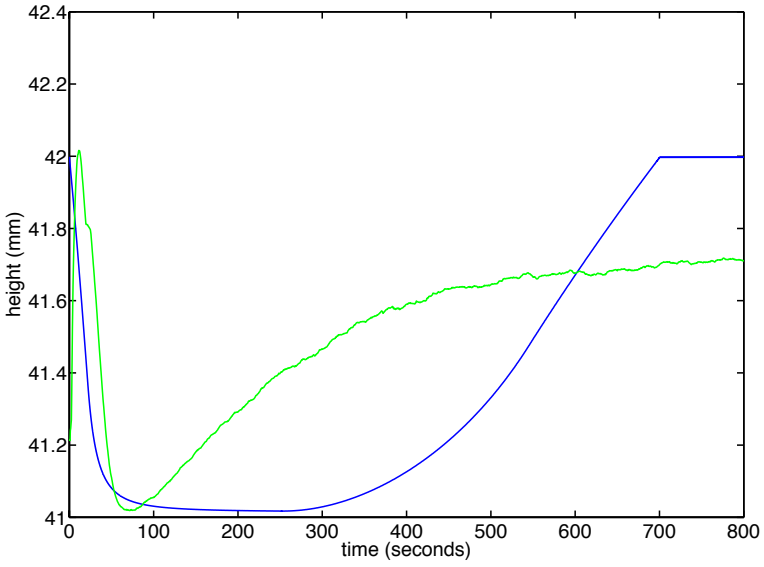

FIGURE 3. The experimentally-measured position $H(t)$ of the top plate and the calculated height $h(t)$ of the sample.

In Fig. 3 we show the time series of the position $H(t)$, together with the result of solving the mathematical initial value problem (25) with exponential shear rate given by fitting the experimental data. Note that the sample initially dilates, as particles start to slide and roll over each other from the initially static configuration. This Reynolds dilatancy occurs on a timescale of about 10 seconds, whereas mixing and segregation occur on a much longer timescale, roughly 100 seconds and 600 seconds, respectively. Since the Gray-Thornton model is not designed to account for the initial transient dilatancy, and the timescales are well separated, we ignore this feature of the experimental time series.

The mathematical solution $\varphi(z,t)$ of (25) is the concentration of small particles on a fixed domain $0 < z < 1$. At each time, the spatial variation of $\varphi(z,t)$ represents a certain volume of the sample, depending on how the local packing depends on the mix of small and large particles. To extract the physical volume from $\varphi(z,t)$, we employ a packing density map $\rho(\varphi)$, based on results from MD simulations and experiments with static packings [5]. The packing density allows us to convert the local small particle concentration into a local effective volume. We integrate the local effective volume over the fixed domain $0 \le z \le 1$ to get the total effective volume of the sample at each time. Since the cross-sectional area of the apparatus is constant, and the initial volume of particles is known, the effective volume generates a height function $h(t)$, which we refer to as the calculated height, shown in Fig. 3. It is this height $h(t)$ that is to be compared to the measured position $H(t)$ of the top plate. Details of the conversion from $\varphi(z,t)$ to $h(t)$ are given in [6].

Both model and experiment exhibit a faster rate for mixing than for segregation, and are in rough qualitative agreement on those rates once the timescale parameter s is set. Two key differences are apparent in Fig. 3: the

resegregation is delayed in the model, and the model predicts complete resegregation in finite time (700 secs. in the figure). Nonetheless, the agreement between model and experiment is remarkable considering that we are using a simple continuum model for a small scale granular system. However, the model naturally fails to capture short-time dilatancy, finite size effects, or three-dimensional effects.

ACKNOWLEDGEMENTS

This research was supported by the National Science Foundation under grants DMS-0604047, and the National Aeronautics and Space Agency under grant NNC04GB086.

REFERENCES

1. N. Giffen and M. Shearer. Shock formation and breaking in particle size-segregation. *J. Discrete and Continuous Dynamical Systems*, submitted, 2009.
2. L. A. Golick and K. E. Daniels. Mixing and segregation rates in sheared granular materials. *Physical Review E*, 80:042301, 2009.
3. J. M. N. T. Gray, M. Shearer, and A. R. Thornton. Time-dependent solutions for particle-size segregation in shallow granular avalanches. *Proceedings of the Royal Society A* , 462(2067):947–972, 2006.
4. J. M. N. T. Gray and A. R. Thornton. A theory for particle size segregation in shallow granular free-surface flows. *Proceedings of the Royal Society A*, 461:1447–1473, 2005.
5. K. D. Kristiansen, A. Wouterse, and A. Philipse. Simulation of random packing of binary sphere mixtures by mechanical contraction. *Physica A*, 358(2-4):249–262, 2005.
6. L. B. H. May, K. C. Phillips, L. A. Golick, M. Shearer, and K. E. Daniels. Shear-driven particle-size segregation of granular materials: comparison of theory, modelling and experiment. Submitted. arXiv:0911.4138 (2009).
7. L. B. H. May, M. Shearer, and K. E. Daniels. Scalar conservation laws with nonconstant coefficients with application to particle size segregation in granular flow. 2009. *J. Nonlinear Science,* submitted, 2009.
8. M. McIntyre, E. L. Rowe, M. Shearer, J. M. N. T. Gray, and A. R. Thornton. Evolution of a mixing zone in granular avalanches. *AMRX*, abm008, 2008.
9. G. D. R. MiDi, European Physical Journal E, 14: 341, 2004.
10. S. B. Savage and C. K. K. Lun. Particle-size segregation in inclined chute flow of dry cohesionless granular solids. *Journal Of Fluid Mechanics*, 189:311–335, 1988.
11. D. Serre. *Systems of Conservation Laws: Geometric structures, oscillations, and initial-boundary value problems*. Cambridge Univ. Press, 2000.
12. M. Shearer, J. M. N. T. Gray, and A. R. Thornton. Stable solutions of a scalar conservation law for particle-size segregation in dense granular avalanches. *European Journal of Applied Mathematics*, 19:61–86, 2008.
13. G.B. Whitham. *Linear and Nonlinear Waves*. Wiley, NY, 1974.